Desalination and Water Treatment
www.deswater.com

doi: 10.1080/19443994.2013.808786

51 (2013) 5035–5048
July

Taylor & Francis
Taylor & Francis Group

Zinc removal from aqueous solutions by adsorption onto bentonite

Karima Bellir*, Mossaab Bencheikh Lehocine, Abdeslam-Hassen Meniai

Laboratoire de l'Ingénierie des Procédés de l'Environnement, Département de Chimie Industrielle, Université Mentouri, Constantine 25000, Algeria
Tel./Fax: +213 31 81 88 80; email: bellir_k@yahoo.fr

Received 31 August 2012; Accepted 26 April 2013

ABSTRACT

Industrial wastewaters contain considerable amounts of metal ions that would endanger public health and the environment if discharged without adequate treatment. The aim of this study is to evaluate, zinc adsorption from aqueous solutions onto Algerian bentonite, kinetics, isotherms and thermodynamic parameters. The characterization of this bentonite was accomplished by using FTIR, TGA and SEM techniques. The effects of contact time, initial metal concentration, agitation speed and temperature were investigated experimentally. The maximum adsorption was reached at pH 8. Pseudo-first-order, pseudo-second-order, Elovich equation, and Intraparticle diffusion models were used to analyze the kinetic data obtained at different concentrations. The pseudo-second-order kinetic model agrees very well with the experimental results. In order to determine the best fit isotherm, in the studied concentration range of Zn^{2+} at 20°C, the experimental equilibrium data were analyzed using four adsorption isotherm models: Langmuir, Freundlich, Temkin and the Redlich–Peterson. The calculated thermodynamic parameters suggested that the adsorption of zinc was physisorptive, spontaneous and endothermic in nature. The results indicate that this bentonite is a suitable adsorbent for the removal of heavy metals especially zinc ions.

Keywords: Heavy metals; Zinc; Adsorption; Bentonite; Kinetic; Isotherm

1. Introduction

Heavy metals are often discharged by a number of industries, such as metal plating facilities, mining operations, tanneries, nuclear power plants, fertilizers and battery productions, this can lead to the contamination of freshwaters and marine environment [1,2].

Heavy metals contained in industrial effluents, constitute a major source of environmental metal pollution, since they are persistent and cannot be degraded nor destroyed but can be biomagnified by aquatic organisms. Toxicity of metal pollution is so slow and interminable [3].

Various treatment approaches have been applied and developed in order to decontaminate heavy metal polluted waters. The most commonly used methods include: oxidation, reduction, chemical precipitation,

*Corresponding author.

Presented at the Conference on Membranes in Drinking and Industrial Water Production.
Leeuwarden, The Netherlands, 10–12 September 2012.
Organized by the European Desalination Society and Wetsus Centre for Sustainable Water Technology

complexation, adsorption, reverse osmosis, ion exchange, solvent extraction, membrane filtration, coagulation, phytoextraction and evaporation, etc [4–7]. Alternatively, adsorption is an important physicochemical process that occurs at the solid-liquid interface and can remove these metals from industrial effluent efficiently and simply [8].

In recent years, a wide variety of materials have been studied as low-cost adsorbents for the removal of heavy metals from water, such as activated carbon, fly ash, lignite, phosphate rock, kaolinite clays, red muds, sawdust, loess soil, etc [9].

The use of clays for the removal of heavy metals found in wastewater has recently been the object of study in many researches due to the uncalculated economical advantages. The cost of clays is relatively low in comparison to other alternative adsorbents. Clays and minerals such as montmorillonite, vermiculite, illite, kaolinite and bentonite are among those natural materials which have been investigated as heavy metal adsorbents. Another advantage of using clay as adsorbent resides in its intrinsic properties, such as high specific surface area, excellent physical and chemical stability, high cation exchange capacity, layered structure [10–12]. Moreover another application of clays (especially montmorillonite and bentonite) is their uses as barriers in landfills to prevent contamination of subsoil and groundwater by leachates containing heavy metals. The utilization of clays as a liner material has been applied for the last few decades, for this reason it is important to study the adsorption of metals by these natural materials.

Taking into account all the above, this study explored the feasibility of utilizing an Algerian thermally treated bentonite for the adsorption of zinc from aqueous solutions. The FTIR, TGA and SEM analyses were done to characterize the adsorbent material. The effects of contact time, initial Zn(II) concentration, agitation speed and pH were investigated using batch adsorption experiments. The suitability of Langmuir, Freundlich, Temkin and Dubinin–Radushkevich adsorption models to the equilibrium data was examined. The kinetic parameters were also calculated to determine rate constants.

2. Experimental materials and methods

2.1. Adsorbent

In this study, bentonite obtained from Maghnia (North-Western part of Algeria) and supplied by ENOF "Enterprise National des substances utiles et des produits non ferreux, Algérie" was used as an adsorbent. The bentonite sample was calcinated at a temperature of 600°C for 2 h in order to increase their mechanical resistance, dehydroxylation and to eliminate some impurities. After heating, the resulting clay was left to cool to room temperature in desiccator.

It was observed that the color of the calcinated clay has changed from grey to brownish. The changing clay color during increasing heat is due to its atomic structural modification.

2.2. Sorbate and chemicals

All chemical reagents procured and applied in this study were of analytical grade and were used without further purification. Stock solution of metal was prepared using zinc sulphate heptahydrate ($ZnSO_4.7H_2O$) in distilled water. Different desired concentrations of Zn^{2+} were prepared by diluting 1,000 mgL^{-1} of the stock solution. The pH of the zinc solutions was kept at set values using nitric acid (HNO_3) and sodium hydroxide (NaOH). For most of the experiments, the pH zinc solutions were adjusted to a pH of 4.5 according to the metal ion species distribution presented in Fig. 7.

2.3. Adsorption experiments

Batch adsorption experiments were performed by contacting 1 g of the calcinated bentonite powder with 100 ml of the zinc aqueous solution of different initial concentrations (1–60 mg/L) at adjusted solution pH (4.5). The experiments were performed in wrist action shaker for a period of 3 h using 250 ml Erlenmeyer flasks at room temperature (20°C). Continuous mixing was provided during the experimental period with a constant agitation speed of 200 rpm for better mass transfer with high interfacial area of contact. All experiments of zinc adsorption were carried out in triplicate at the presence of an electrolyte KNO_3 solution (0.01 M) in order to keep the ionic strength constant. The residual zinc concentration was determined by atomic absorption spectrometry at 213.9 nm maximum wavelength. The amount of metal ions adsorbed in the solid phase (q_t) at each instant of time was obtained by Eq. (1):

$$q_t = \frac{(C_0 - C_t)}{m} \times V \quad (1)$$

where C_0 is the initial concentration of metal ions, C_t is the concentration of metal ions at time t, V is the volume of solution and m mass of clay.

The removal percentage was calculated using the following expression:

$$\text{Removal}\ \% = \frac{C_0 - C_t}{C_0} \times 100 \quad (2)$$

2.4. Analysis and instruments

The concentrations of zinc in the solutions before and after equilibrium were determined by VARIAN Spectra AA-20 plus Atomic Absorption Spectrophotometer. The pH of solution was measured with a HANNA pH meter instrument (HI 8521 N).

The Fourier transform infrared (FT-IR) spectra using KBr pressed disk technique were conducted by Perkin Elmer Spectrum RXI Infrared spectrometer. Calcinated bentonite and KBr were weighted and then were grounded in an agate mortar for 10 min prior to pellet making. The spectra were recorded, in the range of range of 400–4000 cm^{-1}. FT-IR studies of bentonite adsorbent help in the identification of various forms of the minerals present in this clay.

Thermogravimetric analysis was performed using Q50 V6.3 Build 189 TGA Instrument. A mass of 10.71 mg of bentonite was placed in platinum sample holder and heated in air atmosphere up to a temperature of 800°C. The flow rate of nitrogen was 40 ml/min and the heating rate was 5°C/min.

The surface morphology and the microstructural characteristics of clay compounds were analysed using Emission Scanning Electron Microscope (Hitachi S-4700 FEG). The powdered sample, intended for the studies, was covered within a thin layer of chrome in an ionisation chamber.

3. Results and discussion

3.1. Bentonite characterization

3.1.1. FTIR Spectra

FTIR spectra of calcinated bentonite is illustrated in Fig. 1. Positions and assignment of the vibrational bands of this clay are shown in Table 1. The broad and slight bands at 3629.54 and 3456.1 cm^{-1} are due to the O–H stretching vibration of the silanol (Si–OH) groups from the solid and HO–H vibration of the water molecules adsorbed on the silicate surface. The band at 1634.5 cm^{-1} reflects the bending HO–H bond of water molecules, which is retained in the silicate matrix.

The most intensive and sharp band at 1035.5 cm^{-1} represents the Si–O–Si groups of the tetrahedral sheets. Where as the bands around 543.5 and 467 cm^{-1} are ascribed to Si–O–Al (where Al is the octahedral cation) and to Si–O–Si bending vibration. Furthermore, the sharp bands at 794.9 with reflexion at 778.4 cm^{-1} confirm the presence of quartz admixtures in the sample. The picks at 2,851 and 2,917 cm^{-1} are assigned to the aliphatic C–H stretching vibration [13,14].

3.1.2. Thermal analysis of bentonite

TGA analysis of bentonite sample is shown in Fig. 2. It appears that the TGA curve presents two stages of the mass loss. The first step ($T < 180$°C) shows a slight gradual weight loss (about 0.958%). This could be attributed to the removal of adsorbed and interlayer (interstitial) water from the clay

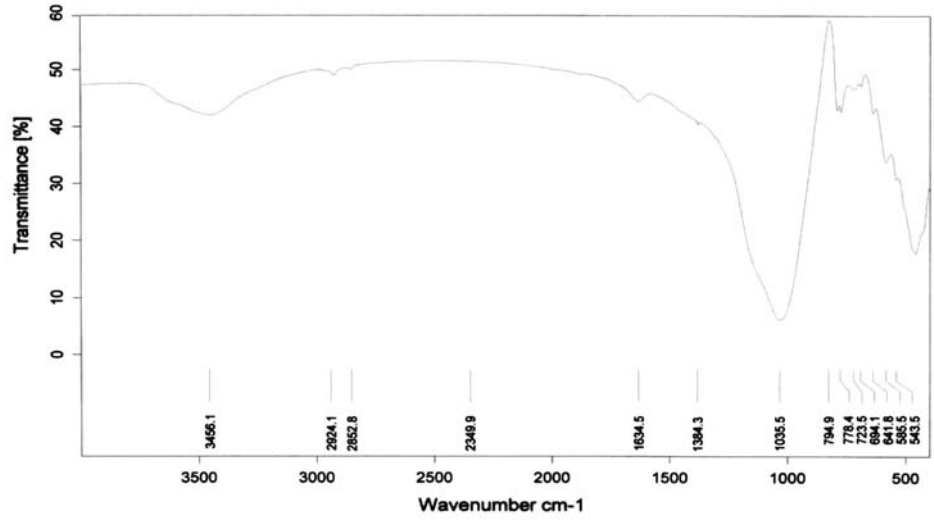

Fig. 1. FTIR spectrum of bentonite sample.

Table 1
FTIR band assignments of calcinated bentonite

Maxima (cm^{-1})	Assignments
3629.54	–OH stretching
3456.1	–OH stretching, hydratation
1634.5	–OH stretching, hydratation
1035.5	Si–O stretching (in plane)
794.9	Quatrz
694.1	Quartz
534.5	Si–O–Al bending
467	Si–O–Si bending vibration

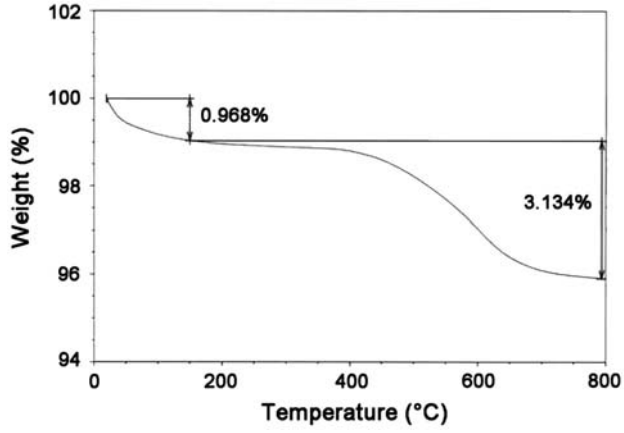

Fig. 2. Thermogravimetric analysis curve of the calcinated bentonite.

mineral. It can also correspond to the elimination of the coordinated water species to the interlayer cations. In the second temperature region, 200–800°C, the weight loss is 3.134% which is due to the loss of hydroxyl groups from clay mineral structure (clay dehydroxylation) [15–17].

3.1.3. Scanning Electron Microscopy

Fig. 3 illustrates the SEM micrograph of a typical thermally treated clay sample at three magnifications. The bentonite particles were mostly irregular in shape and appeared to have randomly arranged pores.

This clay is microporous and shows large number of small flakes. Furthermore the surface morphology of this mineral reveals loose aggregates with severely nonuniform layered structures.

3.2. Effect of operating parameters

3.2.1. Effect of contacting time and initial metal concentration

From an economical point of view, the contact time required to reach equilibrium is an important parameter in waste water treatment. Adsorption of zinc was measured at given contact time (3 h) for five different initial zinc concentrations from 1 to 60 mg/L.

As it is shown in Fig. 4, the plot reveals that the curves are of a saturation type and the chemical equilibrium is attained rapidly. In fact we can notice, that

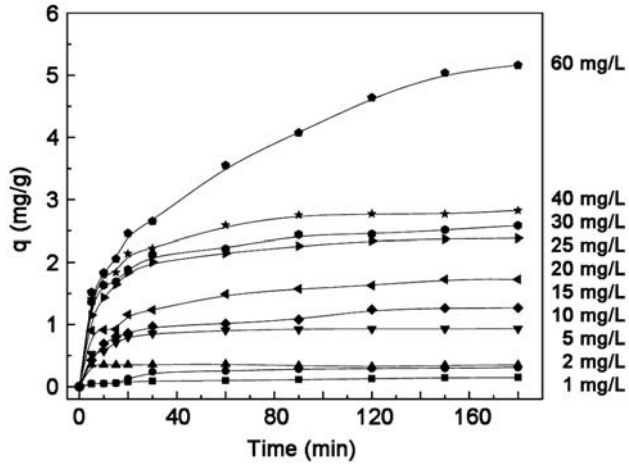

Fig. 4. Effect of contact time and initial concentration on the zinc adsorption by bentonite; Conditions: $v = 200$ rpm, $r = 10$ g/l, $T = 20 \pm 2$°C, pH = 4.5.

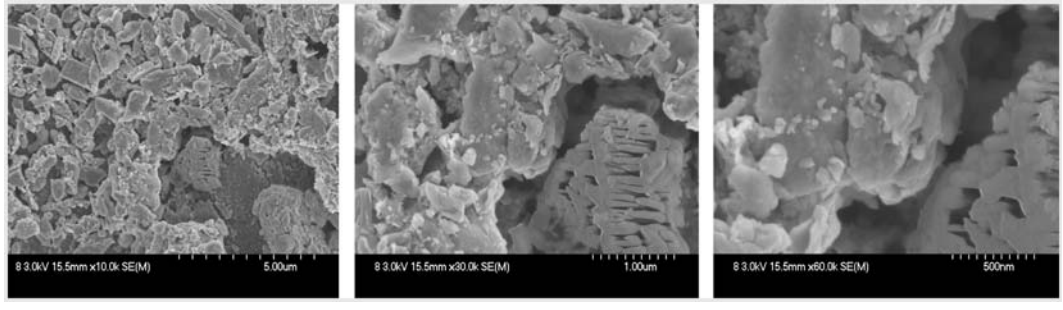

Fig. 3. SEM images of the thermally treated bentonite.

there are two distinct phases, the first one is very short and adsorption is rapid due to the attachment of metal ions to the surface of sorbent and the second is relatively slowing progressively and reached a plateau value at about 60 min. This phenomenon could be attributed to the instantaneous utilization of the most readily available adsorbing sites on the adsorbent surface. The equilibrium was reached within 180 min.

The two stage sorption mechanism with the first rapid and quantitatively predominant and the second slower and quantitatively insignificant, has been extensively reported in literature [18].

The amount of Zn(II) adsorbed at equilibrium increased from 0.15 to 2.82 mgg^{-1} as the initial concentration was increased from 1 to 40 mg L^{-1}. This is a result of the increase in the driving force and the concentration gradient, as an increase in the initial metal concentrations, because the resistance to the metal uptake decreased as the mass transfer driving force increased.

3.2.2. Effect of stirring speed

Because shaking consumes energy and affects the adsorption efficiency, it is important to determine the optimal speed that should be used in wastewater treatment. Experiments were carried out varying the stirring speed between 100 and 600 rpm at zinc concentration of 10 mg/l and stirring time of 3 h and adjusted pH of 4.5.

Below 100 rpm, it was observed, experimentally, that some of the clay particles remained on the base of the beaker and at 700 rpm the magnetic shaker became unstable.

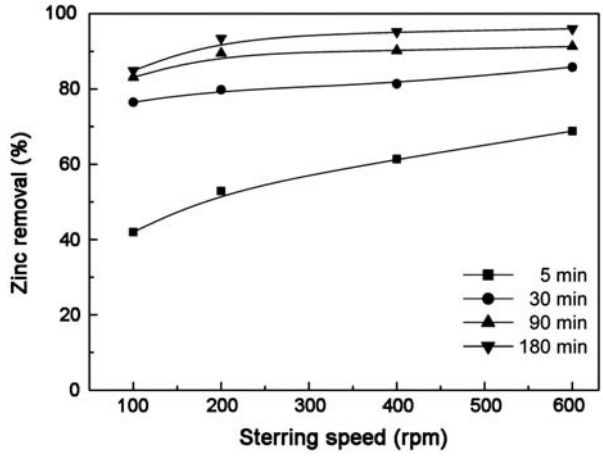

Fig. 5. Effect of agitation speed on the zinc adsorption by bentonite; Conditions: $[Zn^{2+}] = 10$ mg/L, $r = 10$ g/l, $T = 20 \pm 2$°C, pH = 4.5.

Fig. 5 shows the effect of stirring speed on the Zn^{2+} adsorption. As seen, the percentage of metal removal increases depending on the increase of the stirring rate. This observed result is attributed to the improvement in the contact between zinc species in solution and the active sites on the clay, thereby decreasing the thickness of the diffusion layer around the adsorbent surface due to the stirring rate and promoting effective transfer of sorbate ions to the adsorbent site. Furthermore, a higher stirring speed would be propitious to bentonite dispersion.

The effect of stirring speed is most pronounced at the beginning of the adsorption process and becomes negligible when contacting time exceeds 90 min. However, it is clearly seen that the difference in the zinc percentage at 180 min is not very sufficient after 200 rpm value, so 200 rpm was considered as optimal stirring speed for the removal of zinc ions and was selected in the others adsorption experiments. The obtained result is very compatible with the study done by Mellah et al. and Inglezakis et al. [19,20].

3.2.3. Effect of pH

pH is one of the most important environmental factor influencing not only site dissociation, but also the solution chemistry of heavy metals. Hydrolysis, complexation by organic and/or inorganic ligands, redox reactions, precipitation are strongly influenced by pH as well. Moreover, it strongly influences the speciation and the adsorption availability of heavy metals. In fact, the pH value of the solution is an important controlling parameter in the adsorption process. The effect of pH was examined by considering zinc solutions at a pH range of 2–12.

It can be seen from Fig. 6, that the removal rate of Zn^{2+} ions was increased with pH. When the pH value is 8, the adsorption capacity of metal ions was close to saturation, from pH 8 to 12, an adsorption plateau was noticed.

The pH effect was less marked at the end of the adsorption process (after 90 min of shaking time). For high pHs, (alkaline environment) the adsorption was almost unaffected and the corresponding curves were superposed, attaining equilibrium and the maximum adsorption capacity. These results can be explained as follows: At low pH, the negative charges on the bentonite are occupied by H^+ ions, which inhibit the approach of positively charged metal ions, consequently reducing zinc ions binding on the adsorbent surface, causing a decrease in adsorption capacity. In contrast, at high pH level, the competing effect of hydrogen ions decreased and zinc may precipitate and form complexes with OH^-, for example,

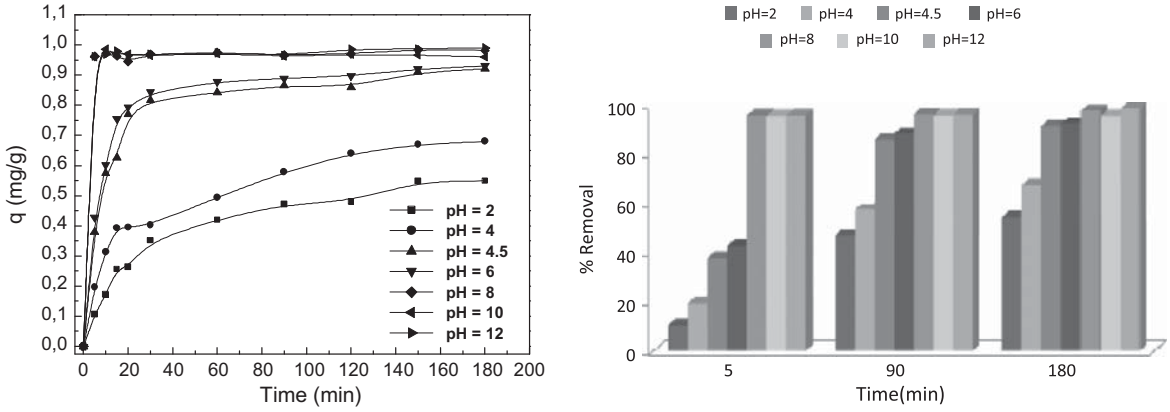

Fig. 6. Effect of pH on the removal of zinc onto bentonite; Conditions: $C_0 = 10\,mg/$, $v = 200\,rpm$, $r = 10\,g/l$, $T = 20 \pm 2$°C.

$Zn(OH)_2$, $Zn(OH)_3^-$, and $Zn(OH)_4^{2-}$. As it is shown in Fig. 2, at pH > 7, the precipitation as $Zn(OH)_2$ plays the main role in removing Zn(II). These results are in agreement with those of Gupta et al. [21], Zhang et al. [22] and Njoku et al. [23].

Measuring the final pHs of the suspension after a contact time of 180 min can give good information for revealing the above comments. Fig. 8 shows the final pH values at the end of the experiments; it can be seen that after zinc retention there is an increase in final pH. However this increase is important at the beginning of the adsorption process, then it varies slightly specially in pH interval of 7–9, consequently H^+ ions may be simultaneously adsorbed with those of zinc. The maximum pH variation was noted at pH = 4.2.

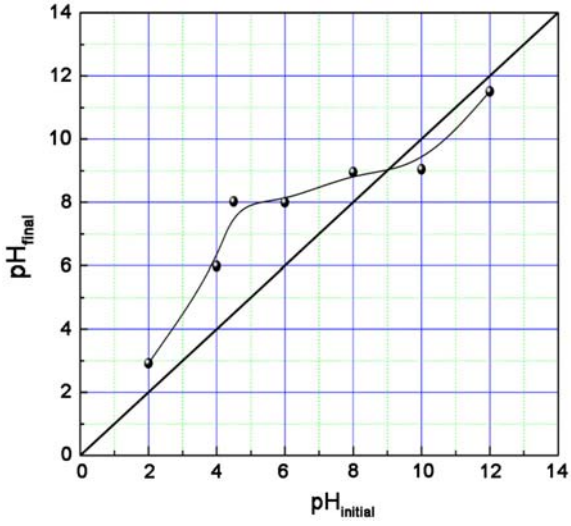

Fig. 8. Dependence between initial pH and final pH.

3.3. Adsorption kinetic models

Adsorption kinetics is one of the important characteristics defining the efficiency of an adsorbent. It describes the solute uptake rate which evidently controls the diffusion process and the residence time of adsorbate uptake at the solid–solution interface. To determine the solute uptake rate and explain the transport of Zn^{2+} to the surfaces of calcinated bentonite, different kinetic models were employed.

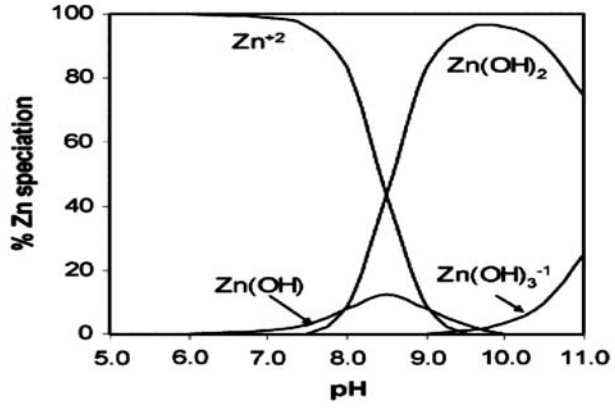

Fig. 7. Distribution of metal ion species of zinc at different pH.

3.3.1. Pseudo-first-order model

Lagergren in 1898 presented a pseudo-first-order rate equation to describe the kinetic process of liquid-solid phase adsorption of oxalic acid and malonic acid onto charcoal, which is believed to be the earliest model pertaining to the adsorption rate based on the adsorption capacity. It is presented as follows [24,25]:

$$\frac{dq_t}{dt} = k_1(q_e - q_t) \tag{3}$$

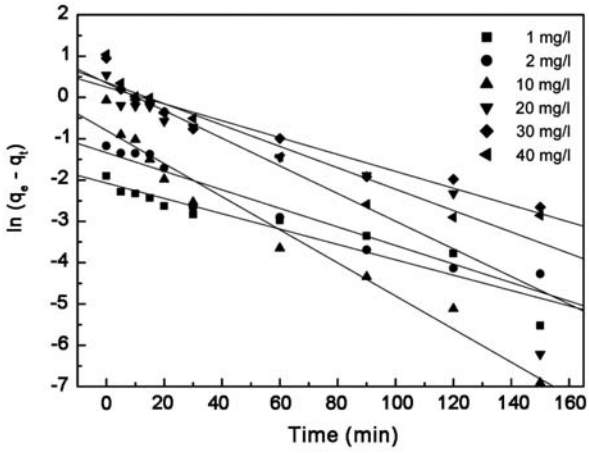

Fig. 9. Pseudo-first-order plot of zinc adsorption onto bentonite at different initial concentrations.

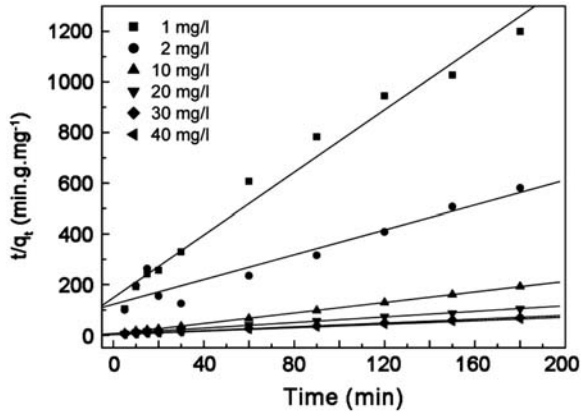

Fig. 10. Pseudo-first-order plot of zinc adsorption onto bentonite at different initial concentrations.

where q_e is the amount of zinc (II) adsorbed at equilibrium (mg/g), q_t is the amount adsorbed at time t (mg/g), k_1 is the rate constant of first order adsorption (min^{-1}). After integration and applying boundary conditions, $t = 0$–t and $q_t = 0$–q_e; the integrated form of Eq. (3) becomes:

$$\ln(q_e - q_t) = \ln q_e - k_1 t \quad (4)$$

Values of adsorption rate constant k_1 for the zinc (II) adsorption onto calcinated bentonite (CB) were determined from the straight line plot of $\ln(q_e - q_t)$ against t (Fig. 9). The data were fitted with a poor correlation coefficient (Table 2), indicating that the rate of removal of zinc onto CB does not follow the pseudo-first-order equation.

3.3.2. Pseudo-second-order model

The pseudo-second-order equation is also based on the sorption capacity of the solid phase. It predicts the behaviour over the whole range of data. Furthermore, it is in agreement with chemisorption being the rate controlling step and is expressed as [26]:

$$\frac{dq_t}{dt} = K_2(q_e - q_t)^2 \quad (5)$$

where k_2 is the rate constant of second order-adsorption (g/mg min). For the same boundary conditions the integrated form of Eq. (5) becomes:

$$\frac{t}{q_t} = \frac{1}{k_2 q_e^2} + \frac{1}{q_e} t \quad (6)$$

The initial sorption rate, h (mg/g min), at $t = 0$ is defined as:

$$h = k_2 q_e^2 \quad (7)$$

where k_2 and h values were determined from the slope and intercept of the plots of t/q_t versus t (Fig. 10). The values of the parameters and correlation

Table 2
Calculated kinetic parameters for pseudo first-order, second order and Elovich kinetic models for the adsorption of zinc onto bentonite

C_0 (mg/l)	$q_{e,\,exp}$ (mg/g)	Pseudo-first-order kinetic			Pseudo-second-order kinetic				Elovich kinetic		
		k_1 (min^{-1})	$q_{e1,\,cal}$ (mg/g)	R^2	k_2 (g/mg min)	h (mg/g min)	$q_{e2,cal}$ (mg/g)	R^2	β (g/mg)	α (mg/g min)	R^2
1	0.15	0.0185	0.1258	0.945	0.2562	6.72×10^{-3}	0.1619	0.979	33.967	0.0202	0.958
2	0.31	0.0224	0.2625	0.930	0.0489	8.18×10^{-3}	0.4088	0.907	11.672	0.0219	0.904
10	0.935	0.0400	0.4496	0.965	0.2255	0.2091	0.963	0.999	8.542	3.0422	0.885
20	1.726	0.0334	1.4214	0.846	0.0475	0.1576	1.8217	0.997	3.707	0.9513	0.957
30	2.585	0.0204	1.2874	0.922	0.0485	0.3414	2.6517	0.999	2.937	2.9370	0.982
40	2.852	0.0258	1.4423	0.921	0.0463	0.3976	2.9296	0.999	2.491	2.4915	0.972

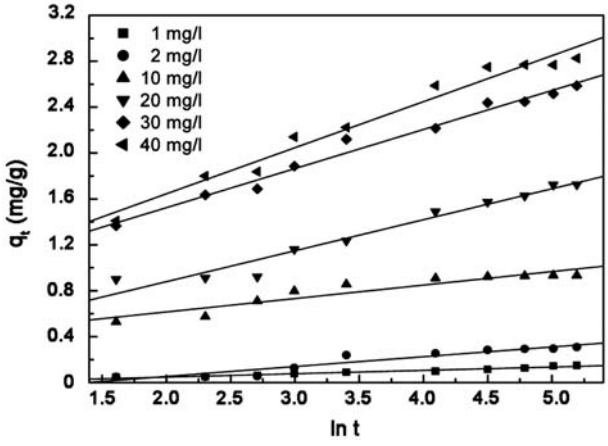

Fig. 11. Elovich kinetic model plot of Zn^{2+} adsorption onto bentonite at different initial concentrations.

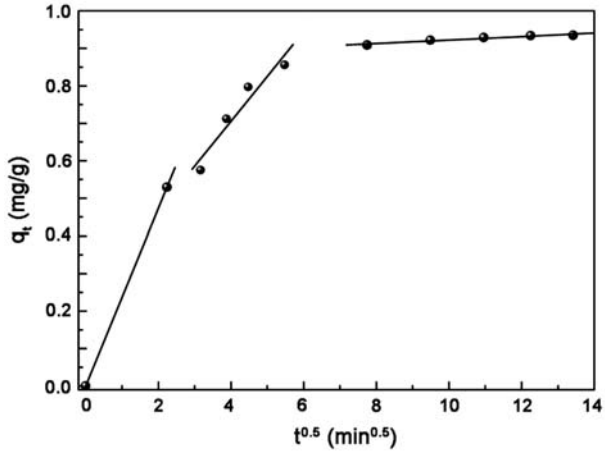

Fig. 12. Intraparticle diffusion plot for Zn^{2+} adsorption onto bentonite; Condition: $C_0 = 10$ mg/l, $v = 200$ tr/min, $r = 10$ g/l, $T = 20 \pm 2$°C, pH ≈ 4.5.

coefficients are also presented in Table 2. The correlation coefficients of all examined data were found very high ($R^2 > 0.98$) excepting for 2 mg/l of initial Zn^{2+} concentration. This shows that the model can be applied for the entire adsorption process and confirms that the sorption of zinc by bentonite is well described by the pseudo-second-order kinetic model.

Elovich model. The Elovich equation was developed to describe the kinetics of chemisorption of a gas onto solids [27]. Elovich model of the sorption process was also tested, it has the following expression:

$$\frac{dq_t}{dt} = \alpha \exp(-\beta q_t) \tag{8}$$

where α (mg g^{-1} min^{-1}) is the initial adsorption rate because (dq_t/dt) approaches α when q_t approaches 0. β (g mg^{-1}) is the desorption constant during any one experiment, related to the extent of the surface coverage and activation energy.

To simplify the Elovich equation, it is assumed that $\alpha\beta t >> 1$ and by applying the boundary conditions $q_t = 0$ at $t = 0$ and $q_t = q_t$ at $t = t$, as given by Eq. (9):

$$q_t = \frac{1}{\beta}\ln(\alpha\beta) + \frac{1}{\beta}\ln t \tag{9}$$

The Elovich kinetic constants, α and β, are obtained from the slope $(1/\beta)$ and the intercept $(1/\beta)$ ln $(\alpha\beta)$ respectively. Fig. 11 represents the application of linear form of Elovich kinetic equation which is a plot of q_t versus ln t. The plot gives linear fit with correlation coefficients in the range of 0.885–0.982. However the values of initial adsorption rate, α, decrease with the increase of initial metal concentration.

Since correlation coefficients are closer to unity (Table 2) for the pseudo-second kinetics more than those of the other kinetic models, the sorption kinetics of adsorption of zinc onto bentonite is better represented by the pseudo-second-order. This suggests that the adsorption system may be chemical or chemisorption nature.

3.4. Adsorption mechanism

Generally, any sorption process can be described by the following three steps: (i) film or surface diffusion, (ii) intraparticle or pore diffusion and (iii) sorption on the interior sites of the sorbent. Since the last step is very rapid, it is assumed that it does not influence the overall kinetics. The rate of adsorption process, therefore, will be controlled by either film diffusion or intraparticle diffusion depending on which step is slower. The Weber–Morris intraparticle diffusion model has often been used to determine if intraparticle diffusion is the rate-limiting step. The intraparticle diffusion equation can be written by following:

$$q_t = k_i t^{1/2} + C \tag{10}$$

where k_i is the intraparticle diffusion constant (mg g^{-1} $min^{0.5}$) and C is the intercept. According to this model, the plot of q_t versus the square root of time $t^{0.5}$ should be linear if intraparticle diffusion is involved in the adsorption process and if the plot passes through the origin then intraparticle diffusion is the sole rate-limiting step. It has also been suggested that in instances when the plot is multilinear two or more steps govern the adsorption process [28–30].

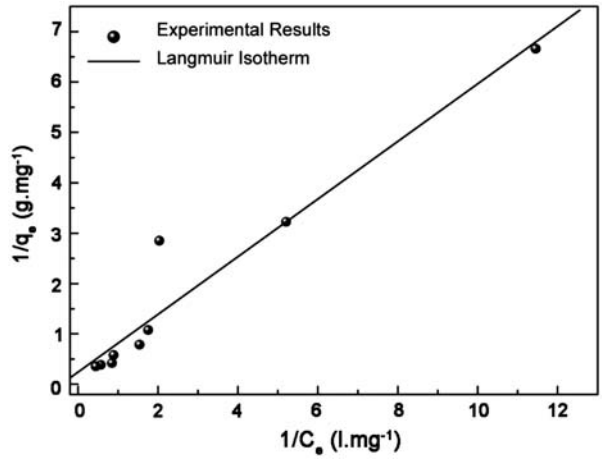

Fig. 13. Linear plot of the Langmuir isotherm of zinc adsorption ofnto bentonite at 20°C.

The plots of q_t versus $t^{0.5}$ have three stage shapes (Fig. 12). The initial first-shape portion of the curve corresponds to the external surface adsorption stage or instantaneous adsorption stage. The second, gradual linear portion corresponds to intraparticle diffusion and the final represents the equilibrium stage. As the plot did not pass through the origin, intraparticle diffusion was not the only rate-limiting step. Thus, there were three processes controlling the adsorption. The intraparticle diffusion constant k_i was calculated from the slope of the second linear section. The value of the intercept C in this second section provides information related to the thickness of the boundary layer. Larger intercepts suggest that surface diffusion has a larger role as the rate-limiting step. The obtained values of k_i and C corresponding to the second section of the curve are $0.1197\,mg\,g^{-1}\,min^{0.5}$ and $0.226\,mg\,g^{-1}$ respectively.

3.5. Adsorption isotherm models

Acquired equilibrium data were fitted to different adsorption isotherm models in order to have insight into the sorption mechanisms, surface properties and affinities of bentonite for Zn^{2+} uptake.

3.5.1. Langmuir isotherm

The theoretical Langmuir sorption isotherm is based on the assumption that the maximum adsorption occurs when a saturated monolayer of solute molecules is present on the adsorbent surface, the energy of adsorption is constant and there is no migration of adsorbate molecules in the surface plane. The Langmuir isotherm model is expressed as follow [31]:

$$q_e = \frac{q_m b C_e}{1 + bC_e} \tag{11}$$

where b is the Langmuir constant ($l\,mg^{-1}$) and q_{max} is the maximum adsorption capacity ($mg\,g^{1}$).

The linearised Langmuir equation applied to the data (Fig. 13) is:

$$\frac{1}{q_e} = \frac{1}{q_m} + \frac{1}{q_m b} \times \frac{1}{C_e} \tag{12}$$

The essential characteristics of the Langmuir isotherm can be expressed in terms of dimensionless constant separation factor or equilibrium parameter, R_L [32] which is defined by Eq. (13):

$$R_L = \frac{1}{1 + bC_0} \tag{13}$$

According to the value of R_L, the isotherm shape can be interpreted as Table 3.

Fig. 14 shows the variation of separation factor (R_L) with initial zinc concentration. It is well observed that the R_L values were in the range of 0.007–0.297, indicating that this adsorption is favourable. Also, the R_L value approaches zero with the increase of C_0 means that the sorption of Zn^{2+} by bentonite is less favourable at high initial zinc concentration.

3.5.2. Freundlich isotherm

In 1906, Freundlich presented the earliest known sorption isotherm equation [3]. This empirical model can be applied to nonideal sorption on heterogeneous surfaces as well as multilayer sorption and is expressed by the following equation:

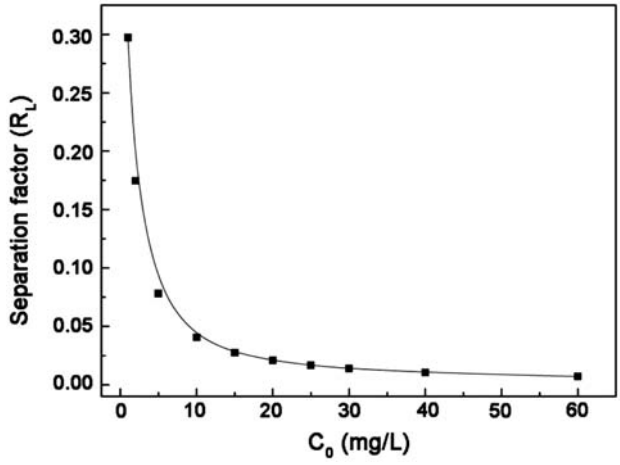

Fig. 14. Variation of the Langmuir separation factor (R_L) as a function of initial zinc concentration.

Table 3
Langmuir isotherm constant parameter, R_L

R_L value	Type of isotherm
$R_L > 1$	Unfavorable
$R_L = 1$	Linear
$R_L = 0$	Irreversible
$0 < R_L < 1$	Favorable

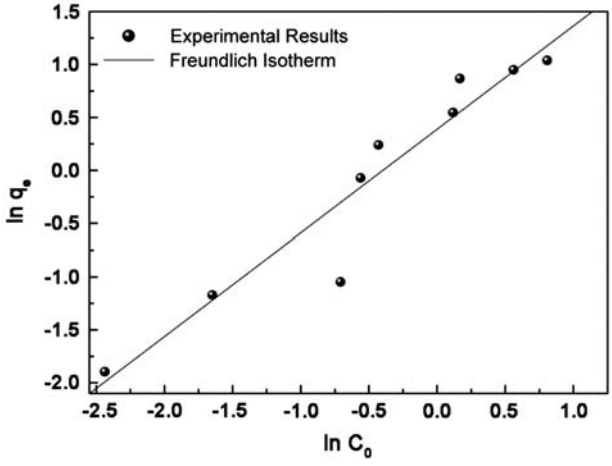

Fig. 15. Linear plot of Freundlich isotherm of zinc sorption onto bentonite at 20°C.

$$q_e = K_F C_e^{\frac{1}{n}} \quad (14)$$

where C_e (mg/L) is the equilibrium concentration and q_e (mg/g) is the amount adsorbed of zinc per unit mass of the adsorbent. The constant n is the Freundlich equation exponent that represents the parameter characterizing quasi-Gaussian energetic heterogeneity of the adsorption surface [34]. K_F ($mg^{1-(1/n)} L^{1/n}/g$) is the Freundlich constant indicative of the relative adsorption capacity of the adsorbent.

The Freundlich exponent, n, should have values lying in the range of 1–10 for classification as favorable adsorption [33]. The linear form of this model is given by Eq. (15):

$$\ln q_e = \ln K_F + \frac{1}{n} \ln C_e \quad (15)$$

Fig. 15 shows the linear plot of Freundlich isotherm of Zn(II) sorption onto bentonite at 20°C. Values of K_F and n are calculated from the intercept and slope of the plot and are presented in Table 2.

According to [35], n value between 1 and 10 shows easy separation beneficial adsorption. This also indicates high affinity of the adsorbent to the metal ions. Therefore, this means that the adsorption of Zn was favorable by the Freundlich isotherm. The values of n have also been reported to be related to the distribution of bonded ions on the sorbent surface.

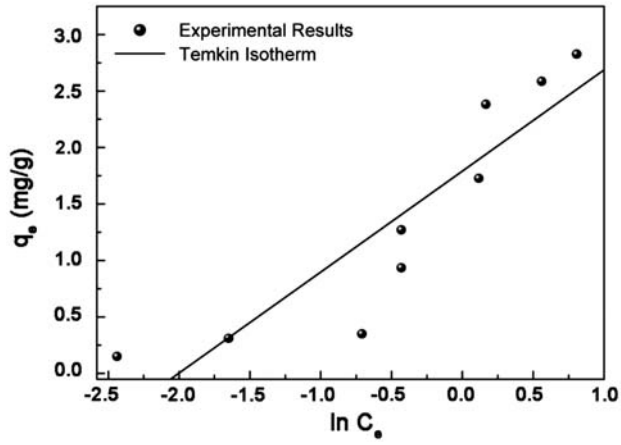

Fig. 16. Linear plot of Temkin isotherm for zinc sorption onto bentonite at 20°C.

3.5.3. Temkin isotherm

The derivation of the Temkin isotherm assumes that the fall in the heat of sorption is linear rather than logarithmic, as implied in the Freundlich equation [36]. The Temkin isotherm has generally been applied in the following form [37]:

The Temkin isotherm equation as given by Malkoc and Nuhoglu [38] is:

$$q_e = \frac{RT}{b} \ln(AC_e) \quad (16)$$

$$q_e = B \ln A + B \ln C_e \quad (17)$$

where $B = (RT/b)$; q_e ($mg\,g^{-1}$) and C_e ($mg\,L^{-1}$) are the amount adsorbed at equilibrium and the equilibrium concentration, respectively. Also T is the absolute temperature (K) and R is the universal gas constant. The constant b is related to the heat of adsorption. The isotherm plot for the sorption of the metal ions is shown in Fig. 16. The isotherm constants were obtained from the intercepts and slopes and are shown in Table 4.

3.5.4. Dubinin Raduskevich isotherm

Another popular equation for the analysis of isotherms of a high degree of regularity is that proposed

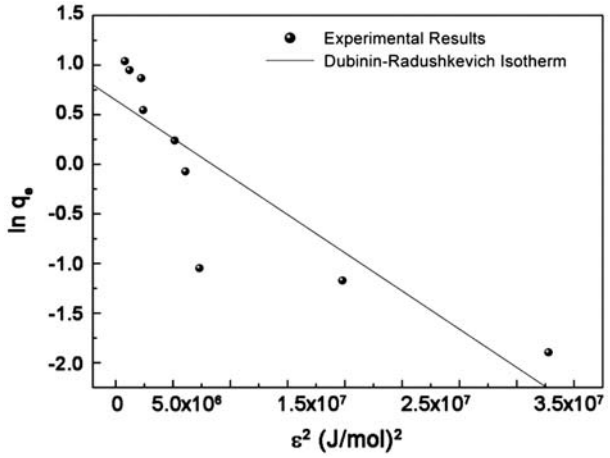

Fig. 17. D–R isotherm plot of zinc sorption onto bentonite at 20°C.

Table 4
Langmuir, Freundlich, Temkin, and the D–R isotherm model constants and correlation coefficients for sorption of zinc onto bentonite

Isotherm	Parameters
Langmuir	
q_m (mg/g)	1.7471
b (L/mg)	2.3642
R^2	0.9322
Freundlich	
K_F ($mg^{1-(1/n)} L^{(1/n)}/g$)	1.4747
n	1.0245
R^2	0.9158
Temkin	
A (L/g)	7.444
B	0.8998
R^2	0.8263
Dubnin–Raduchkivich	
q_m (mol/g)	1.9115
E (kJ/mol)	2.5482
R^2	0.7713

by Dubinin. They have reported that the characteristic sorption curve is related to the porous structure of the sorbent [39]. The isotherm is as follows:

$$q_e = q_m \exp(-\beta\varepsilon^2) \quad (18)$$

The linear form (Fig. 17) of the equation is given as:

$$\ln q_e = \ln q_m - \beta\varepsilon^2 \quad (19)$$

where q_e, the equilibrium solid phase concentration; q_m, the theoretical saturation capacity and: The Polanyi potential given as:

$$\varepsilon = RT \ln\left(1 + \frac{1}{C_e}\right) \quad (20)$$

β is a constant related to the adsorption energy by Eq. (20).

The sorption mean free energy is the energy required to transfer one mole of the sorbate from infinity in solution to the surface of solid. The magnitude of the sorption mean free energy E is widely used for estimating the type of adsorption.

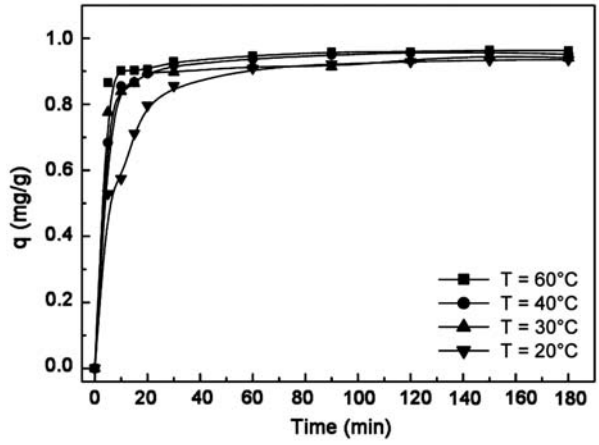

Fig. 18. Effect of temperature on the adsorption of zinc.

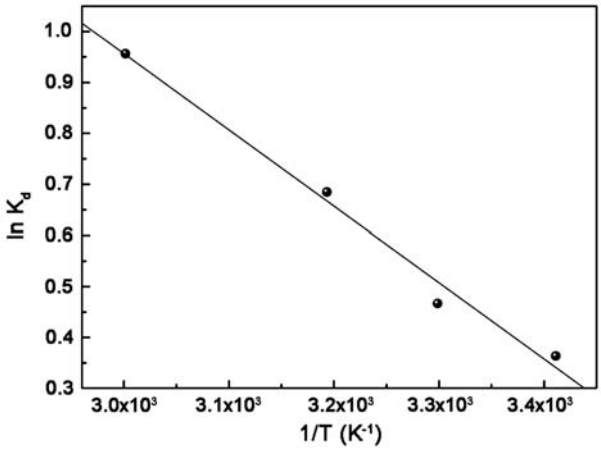

Fig. 19. Linear plot of the thermodynamic study.

$$E = \frac{1}{(2\beta)^{\frac{1}{2}}} \quad (21)$$

It has been reported in several other researchers on the mean sorption energy being $< 8\,kJ\,mol^{-1}$ depicting physical sorption, between 8–16 $kJ\,mol^{-1}$ showing chemical ion-exchange and above 40 $kJ\,mol^{-1}$ showing chemisorption mechanism [40]. The E value was found equal to 2.8452 kJ/mol, indicating that the type of sorption of zinc onto bentonite is essentially physical. As seen in Table 4, the Langmuir model was very suitable for describing the sorption equilibrium of Zn^{2+} onto bentonite.

3.6. Thermodynamic study

The effect of temperature on the adsorption of Zn (II) by bentonite was studied from 20 to 60°C using 10 mg/L initial zinc concentration at pH = 4.5. It was shown that an increase in the metal adsorption rate resulted in increasing of temperature indicating the process to be endothermic (Fig. 18).

The thermodynamic parameters of the adsorption process provide a better understanding of the effects of temperature. They are determined by employing the following equations:

$$K_d = \frac{q_e}{C_e} \quad (22)$$

$$\Delta G = -RT \ln K_d \quad (23)$$

$$\ln K_d = \frac{\Delta S}{R} - \frac{\Delta H}{RT} \quad (24)$$

Fig. 19 shows that ln K_d had a linear relationship with $1/T$ with a R^2 value of 0.9872. The slope and intercept are $-\Delta H/R$ and $\Delta S/R$, respectively, and ΔH and ΔS were determined to be 12.45 $kJ\,mol^{-1}$ and 1.49 $kJ\,mol^{-1}\,K^{-1}$. ΔH was positive, and it indicated that the adsorption of Zn^{2+}onto the calcinated bentonite was endothermic and physical in nature, this confirms the results aforementioned in Section 3.5.4. ΔS was also positive, and this meant an irregular increase of the randomness at the clay-solution interface during adsorption procedure. The results of Gibbs free energy (ΔG) were listed in Table 5. ΔG was negative at all four temperatures. ΔG decreased with the increase of temperature. It suggested that the adsorption of Zn^{2+} onto the bentonite was a spontaneous procedure, the spontaneous degree become greater with the increase of temperature. Increasing temperature is beneficial to the adsorption procedure. Similar results were also reported by Nassem et al. [41] and Bhattacharyya et al. [42].

Table 5
Thermodynamic parameters of zinc adsorption onto bentonite

Temperature (°C)	ΔG ($kJ\,mol^{-1}$)	ΔH ($kJ\,mol^{-1}$)	ΔS ($J\,mol^{-1}\,K^{-1}$)
20	−0.8303		
30	−1.2833	12.4494	0.0453
40	−1.7362		
60	−2.6423		

4. Conclusion

The present study has evaluated the zinc (II) ions removal potential of *an Algerian thermally treated bentonite*. Various forms of the minerals present in this clay have been identificated by FTIR technique. The morphological heterogeneity of the sample was observed in the SEM image. Bentonite has presented two steps of weight loss.

The results showed that the adsorption process depended significantly on contacting time, stirring speed, temperature and solution pH. At higher pH values, zinc removal was tended to be a combination of adsorption, precipitation and complexation.

Adsorption zinc kinetic onto bentonite has been better described by the pseudo-second-order kinetic model. The adsorption process follows Langmuir isotherm model. The obtained values of the separation factor R_L has given an indication of favorable adsorption.

The thermodynamic calculations have shown that the process was endothermic. The negative value of the Gibbs energy change of the adsorption indicates that the zinc adsorption was spontaneous and physic in nature.

In conclusion, bentonite can be expected to become a good cost-effective adsorbent for removing heavy metals from wastewater.

Symbols

A — Temkin constant, L/g
B — Temkin constant
b — Langmuir constant, L/mg
C_e — equilibrium concentration of Zn^{2+} solution, mg/L
C_t — zinc concentration at time t, mg/L
C_o — initial concentration of Zn^{2+} solution, mg/L
h — initial adsorption rate, $mg\,g^{-1}\,min^{-1}$
K_d — equilibrium constant, L/g
K_F — Freundlich constant, $mg^{1-(1/n)}\,L^{1/n}/g$

k_i — intraparticle diffusion constant, $mg\,g^{-1}\,min^{-0.5}$
k_1 — rate constant of pseudo-second-order adsorption, min^{-1}
k_2 — rate constant of the pseudo-first-order adsorption process, $g\,mg^{-1}\,min^{-1}$
m — adsorbent mass, g
n — Freundlich constant
q_e — amount of zinc adsorbed per unit mass of adsorbent at equilibrium, mg/g
q_m — maximum adsorption capacity mg/g
q_t — amount of zinc adsorbed per unit mass of adsorbent at time t, mg/g
r — solid–liquid ratio, g/l
R — gas constant, 8.314 J/mol/K
R_L — separation factor or equilibrium parameter
t — time, min
T — absolute temperature, K
v — agitation speed, rpm
V — volume of the solution, L

Greek

α — initial adsorption rate, $mg\,g^{-1}\,min^{-1}$
β — desorption constant, $g\,mg^{-1}$
ε — Polanyi potential
ΔG — change in Gibbs free energy, kJ/mol
ΔH — change in Enthalpy, kJ/mol
ΔS — change in Entropy, kJ/mol K

References

[1] K.S. Low, C.S. Lee, Sorption of cadmium and lead from aqueous solutions by spent grain, Process Biochem. 36 (2000) 59–64.
[2] S.E. Bailey, T.J. Olin, R.M. Bricka, A review of potentially low-cost sorbents for heavy metals, Water Res. 33 (1999) 469–2479.
[3] S. Veli, B. Alyuz, Adsorption of copper and zinc from aqueous solutions by using natural clay, J. Hazard. Mater. 149 (2007) 226–233.
[4] D. Mohan, K.P. Singh, Single- and multi-component adsorption of cadmium and zinc using activated carbon derived from bagasse fan agricultural waste, Water Res. 36 (2002) 2304–2318.
[5] T. Akar, S. Tunali, I. Kiran, Botrytis cinerea as a new fungal biosorbent for removal of Pb(II) from aqueous solutions, Biochem. Eng. J. 25 (2005) 227–235.
[6] A. Sarı, M. Tuzen, D. Çıtak, M. Soylak, Equilibrium, kinetic and thermodynamic studies of adsorption of Pb(II) from aqueous solution onto Turkish kaolinite, J. Hazard. Mater. B 149 (2007) 283–291.
[7] J.W. Patterson, Industrial Waste Water Treatment Technology, Science, New York, 1997.
[8] S. Veli, B. Alyuz, Adsorption of copper and zinc from aqueous solution by using natural clay, J. Hazard Mater. 149 (2007) 226–233.
[9] S. Xing, M. Zhao, Z. Ma, Removal of heavy metal ions from aqueous solution using red loess as an adsorbent, J. Environ. Sci. 23(9) (2011) 1497–1502.
[10] K.G. Bhattacharyya, S.S. Gupta, Adsorption of a few heavy metals on natural and modified kaolinite and montmorillonite: A review, Adv. Colloid Interface Sci. 140(2) (2008) 114–131.
[11] V.R. Ouhadi, R.N. Yong, M. Sedighi, Desorption response and degradation of buffering capability of bentonite, subjected to heavy metal contaminants, Eng. Geol. 85(1–2) (2006) 102–110.
[12] T.K. Sen, D. Gomez, Adsorption of zinc (Zn^{2+}) from aqueous solution on natural bentonite, Desalination 267 (2011) 286–294.
[13] Z.P. Tomić, S.B. Antić Mladenović1, B.M. Babic, Modification of smectite structure by sulfuric acid and characterization of the modified smectite, J. Agric. Sci. 56(1) (2011) 25–35.
[14] B. Tyagi, C.D. Chudasama, R.V. Jasra, Determination of structural modification in acid activated montmorillonite clay by FT-IR spectroscopy, Spectrochim. Acta, Part A 64 (2006) 273–278.
[15] M. Gourouza, I. Natatou, A. Boos, Physico-chemical characterization of Sabon-Karré's clay, J. Mater. Environ. Sci. 2(4) (1999) 415–422.
[16] F. Ayari, E. Srrasra, M. Trabelsi-Ayadi, Characterization of bentonite clays and their use as adsorbent, Desalination 185 (2005) 391–397.
[17] F. Kooli, Exfoliation properties of acid-activated montmorillonites and their resulting organoclays, Langmuir 25 (2009) 724–730.
[18] C. Yang, J. Wang, M. Lei, Biosorption of zinc (II) from aqueous solution by dried activated sludge, J. Environ. Sci. 22(5) (2010) 675–680.
[19] A. Mellah, S. Chegrouche, The removal of zinc from aqueous solutions by natural bentonite, Water Res. 30(3) (1997) 621–629.
[20] V.J. Inglezakis, M.A. Stylianou, D. Gkantzou, Removal of Pb (II) from aqueous solutions by using clinoptilolite and bentonite as adsorbents, Desalination 210 (2007) 248–256.
[21] V.K. Gupta, A. Rastogi, V.K. Saini, N. Jain, Biosorption of copper (II) from aqueous solutions by Spirogyra species, Colloid Interface Sci. 296 (2006) 59–63.
[22] H. Zhang, Z. Tong, T. Wei, Removal characteristics of Zn(II) from aqueous solution by alkaline Ca-bentonite, Desalination 267 (2011) 103–108.
[23] V.O. Njoku, E.E. Oguzie, C. Obi, Adsorption of copper (II) and lead (II) from aqueous solutions onto a Nigerian natural clay, Aust. J. Basic Appl. Sci. 5(5) (2011) 346–353.
[24] S. Lagergren, About the theory of so-called adsorption of soluble substances. Kungliga Svenska etenskapsakademiens, Handlingar 24(4) (1898) 1–39.
[25] H. Qiu, L. Lv, B.C. Pan, Critical review in adsorption kinetic models, J. Zhejiang Univ. A 10(5) (2009) 716–724.
[26] Y.S. Ho, G. McKay, The kinetics of sorption of divalent metal ions onto sphagnum moss peat, Water Res. 34(3) (2000) 735–742.
[27] Y.S. Ho, G. McKay, Sorption of copper (II) from aqueous solution by peat, Adsorpt. Sci. Technol. 20(8) (2002) 797–813.
[28] Y.S. Ho, Citation review of Lagergreen kinetic rate equation on adsorption reaction, Scientometrics 59(1) (2004) 171–177.
[29] M.A. Al Ghouti, M.A.M. Khraisheh, Adsorption behaviour of methylene blue onto Jordanian diatomite: A kinetic study, J. Hazard. Mater. 165 (2009) 589–598.
[30] H.K. Boparai, M. Joseph, Kinetics and thermodynamics of cadmium ion removal by adsorption onto nano zerovalent iron particles, J. Hazard. Mater. 186 (2011) 458–465.
[31] I. Langmuir, The adsorption of gases on plane surfaces of glass, mica and platinium, J. ACS 40 (1918) 1361–1403.
[32] K.R. Hall, L.C. Eagleton, A. Acrivos, T. Vermeulen, Pore and solid-diffusion kinetics in fixed-bed adsorption under constant-pattern conditions, Ind. Eng. Chem. Fundam. 5(12) (1966) 212–223.
[33] H.M.F. Freundlich, Over the adsorption in solution, J. Phys. Chem. 57 (1906) 385–470.
[34] R.C. Bansal, M. Goyal, Activated Carbon Adsorption, CRC Press, Taylor Francis Group, Boca Raton, FL, 2005.

[35] K. Kadrivelu, C. Namasiayam, Agricultura by-products as metal adorbents onto coir-pith carbon, Environ. Technol. 21 (2000) 1091–1097.
[36] C Aharoni, D.L. Sparks, Kinetics of soil chemical reactions – A theoretical treatment, in: D.L. Sparks, D.L. Suarez (Eds.), Rates of Soil Chemical Processes, Soil Science Society of America, Madison, WI, 1991, pp. 1–18.
[37] C. Aharoni, M. Ungarish, Kinetics of activated chemisorption. Part 2. Theoretical models, J. Chem. Soc. Far. Trans. 73 (1977) 456–464.
[38] E. Malkov, Y. Nuhoglu, Determination of the kinetic and equilibrium parameters of the batch adsorption of Cr(VI) onto waste acorn of quercus ithaburensis, Chem. Eng. Process 46 (2007) 1020–1029.
[39] M.M. Dubinin, The potential theory of adsorption of gases and vapors for adsorbents with energetically non-uniform surface, Chem. Rev. 60 (1960) 235–266.
[40] M. Horsfall, A.I. Spiff, Studies on the influence of mercaptoacetic acid (MAA) modification of Cassava (*Manihot sculenta cranz*) waste biomass on the adsorption of Cu^{2+} and Cd^{2+} from aqueous solution, Bull. Korean Chem. Soc. 25 (2004) 969–976.
[41] R. Naseem, S.S. Tahir, Removal of Pb(II) from aqueous/acidic solutions by using bentonite as an adsorbent, Water Res. 35 (6) (2001) 3982–3986.
[42] K.G. Bhattacharyya, S.S. Gupta, Adsorption of chromium(VI) from water by clays, Ind. Eng. Chem. Res. 45(21) (2006) 7232–7240.